Egypt. J. Chem. **Vol. 67**, No. 8. pp. 137 - 155 (2024)

Egyptian Journal of Chemistry

http://ejchem.journals.ekb.eg/

Evaluation of corrosion and wear features of Al matrix reinforced with particles ($SiC+Y_2O_3$) coated with either nano-Ag/Ni or nano/Ag/Cu

Ghada Fadel[a], Lamiaa Z. Mohamed[b,*], Ghalia A. Gaber[c], Omayma A. Elkady[d], Aiea A. Elhabak[a], Mahmoud A. Adly[a],Shimaa A. Abolkassem[d]

[a] Mechanical Design and Production Engineering Department, Faculty of Engineering, Cairo University, Giza, 12613, Egypt

[b] Mining, Petroleum, and Metallurgical Engineering Department, Faculty of Engineering, Cairo University, Giza, 12613, Egypt

[c] Department of Chemistry, Faculty of Science (Girls), Al-Azhar University, Yousef Abbas Str., Nasr City, P.O. Box: 11754, Cairo, Egypt

[d] Powder Technology Division, Manufacturing Technology Institute, Central Metallurgical Research and Development Institute, Helwan El-Tabbin, P.O. Box 87, Cairo, Egypt

Abstract

A new generation of Al-hybrid composite was successfully fabricated using the powder metallurgy technique after the electroless chemical deposition of both nano Ni and Cu on the surface of Y_2O_3-SiC mixture particles. Al metal matrix (AMM) was reinforced with nano-Ag/Ni or nano-Ag/Cu coated ($SiC-Y_2O_3$) particles with 2.5, 5, and 7.5 wt% content by a 50:50 ratio of SiC to Y_2O_3. The microstructure was examined by optical, SEM, EDX, and TEM. The XRD also was used for phase identification. A wettability test was established on the sintered samples. The wear behavior was conducted. Evaluation of the corrosion feature of the AMM reinforced with ($SiC+Y_2O_3$)/ either nano-Ag/Ni or nano-Ag/Cu was investigated in 3.5% NaCl. The inhibiting impact in 3.5% NaCl solution was studied by potentiodynamic polarization (PDP). The AMM reinforced with ($SiC+Y_2O_3$)/nano-Ag/Cu has a good mixed-type corrosion inhibitor. Also, the corrosion rate decreased by increasing either nano-Ag/Ni or nano-Ag/Cu. The protecting film was formed on the AMM reinforced by either nano-Ag/Ni or nano-Ag/Cu and confirmed by SEM and EDX.

Keywords: Al matrix reinforced; Powder metallurgy; Wear behavior; Corrosion resistance; Microstructure, Wettability.

.

1. Introduction

Metal matrix composites (MMCs) are a sort of composite material where the reinforced matrix is a metal like Al, Mg, Cu…etc. Typical types of reinforcements that are used in MMCs are ceramic materials such as SiC and Al_2O_3 which can remarkably improve the material's strength, hardness,

*Corresponding author e-mail: lamiaa.zaky@cu.edu.eg; (Lamiaa Z. Mohamed).
Received date 10 November 2023; revised date 08 January 2024; accepted date 04 February 2024
DOI: 10.21608/EJCHEM.2024.247764.8845

and wear resistance [1]. Aluminum metal matrix composites (AMMCs) are among the most used metal matrix composites. AMMCs have been utilized by the automotive industries, aerospace, and other fields because of their excellent mechanical, tribological, and physical properties compared to traditional aluminum alloys which have low hardness and poor wear resistance [2]. AMMCs have been reinforced by various types of ceramics which all serve different purposes depending on the type of application they were intended for, and the kind of properties expected from them. However, some of these types were more utilized than others due to their better physical and mechanical properties, making them suitable -with little adjustments- for various applications such as SiC [3, 4]. The SiC is considered one of the most used ceramics as a reinforcement for AMMCs but it provides the more ductile Al-matrix with the necessary strength. Many studies found that the ceramic/metal interface needed modification to better bond the ceramic phase and the Al-matrix. The main cause of coating SiC particles with Cu is to prevent the reaction between Al and SiC particles to produce phases or compounds [5]. Hybrid composites improve performance than single-reinforced composites. The hybrid composite's net product depends greatly on the selection of the matrix and reinforcements. Also, the reinforcement weight percentage, their size, the interfacial interaction between them and the matrix material, and the fabrication method [6, 7, 8].

SiC and Al_2O_3 have been widely used reinforcement materials for mechanical and tribological applications due to their excellent strength and wear resistance [9, 10, 11]. However, more recently, there has been a growing interest in Y_2O_3 as a reinforcing phase due to its more stable nature as a rare earth oxide compared to Al_2O_3, making it a better candidate for the sintering process in hybrid AMMCs [12]. The result of grain size measurement revealed Y_2O_3 particulates to be more effective than Al_2O_3 particulates in grain boundary pinning and they suggested that the plausible reason could be its excellent thermal stability [13, 14, 15]. The surface modification of the ceramic particles is necessary for improving the interfacial bonding in the composite material. However, coating the ceramic particles using the electroless deposition technique with either Ni or Cu is widely preferred because of its overall lower cost and ability to develop coat layers with uniform thickness on the reinforcement phase surface [16]. It studied the effect of different consolidation techniques on the properties of AMMCs reinforced with Ni or Cu-coated SiC with an electroless deposition technique [17, 18]. This work aims at manufacturing a new generation of composite material from the AMM-reinforced particles ($SiC+Y_2O_3$) coated with nano-Ag/Ni or nano-Ag/Cu for mechanical applications and improving the corrosion and wear behaviors of the consolidated samples, which are used for manufacturing spare parts suitable for sports devices. Which require high corrosion and wear resistance.

2. Experimental work

2.1. Materials

The Al, SiC, and Y_2O_3 were bought with a purity of 99.99%, 99.9%, and 99%, respectively. Powders were supplied from DOP ORGANIC KIMYA SAN. VE TIC.LTD.STI. Ostim. Ankara. Turkiye. The manufacturing of hybrid AMMCs was mentioned in our previous work [19]. Powder metallurgy (PM) is commonly used as a segregation effect, and intermetallic phase formation is lower in these

processes than in casting [20]. The microstructure, tribological, and chemical properties of hybrid AMMCs reinforced with particles ($SiC+Y_2O_3$) coated with nano-Ag/Ni or nano-Ag/Cu were studied. The mixed SiC and Y_2O_3 powders were coated with nano-Ag/Ni or nano-Ag/Cu layers using the electroless chemical deposition technique before their addition to the AMM. The coating was applied to wettability between the ceramic particles and the metal matrix and to prevent un undesirable Al_3C_4 phase formation. Cold pressing technique and vacuum sintering were used for the manufacturing process. The microstructure displays that Al particles have irregular shapes, with a particle size that ranges from 1 to 5 µm, while SiC particles have an irregular shape with particle size ranging from 1 to 10 µm, and lastly, Y_2O_3 particles also have irregular shapes but with a particle size that ranges from 650 nm to 10 µm [19]. Two batches of Al/($50SiC-50Y_2O_3$) composites were prepared. Electroless deposition baths are used to coat the ($SiC-Y_2O_3$) powders in the first batch with nano-Ag/10 wt% Ni and the second with nano-Ag/10 wt% Cu. Each group of coated powders was then mixed with the Al powder as a matrix with 2.5, 5, and 7.5 wt%. The powders are then compacted by the uniaxial press under 480Mpa and then sintered at 600 ^oC for 1 h in a vacuum furnace. The density of all samples was estimated according to Archimedes' principle. Also, both macro and microhardness were estimated.

2.2 Characterization of powders and sintered samples

Transmission electron microscopy (TEM) investigated the coated reinforcement particles using the TEM device, model Talos F200i S. An optical tensiometer model Theta Flow was used to measure their contact angles by applying a sessile drop test to study the wettability of the composite samples and the effect of different coatings on the interfacial bonding. All sintered samples were ground by SiC papers up to 1200 grit, then the specimens were polished using alumina paste. The microstructure of polished samples was studied using a scanning electron microscope (SEM) model (QUANTA FEG250, Holland) with energy-dispersive X-ray analysis (EDX). For phase identification of the sintered samples, the X-ray diffraction (XRD) technique was utilized using an X-ray diffractometer (model x, pert PRO PANalytical) with Cu kα radiation (λ= 0.115406 nm). This is estimated in the previous work [19]. Hardness and microhardness were measured for the sintered samples with an average of 5 readings at 500 gm load. A pin-on-disc tribometer was used to measure the wear rate (WR) of the prepared samples according to ASTM G99-95 standard. A stainless-steel disc of 304 grade was used, and a load of 10N with a running time of 5 min for each specimen was applied. AMMC samples were tested at three different sliding speeds of 0.5, 1, and 1.5 m/s to study the effect of different weight percentages of the reinforcement materials on the WR.

The electrochemical studies were achieved by three-electrode cell Potentiostat/Galvanostat PGZ 301. VoltaMaster 4 software connected to a computer fitting the obtained data. AMMC with ($SiC+Y_2O_3$) coated with either nano-Ag/Ni or nano-Ag/Cu is the working electrode with an exposed area of 1 cm^2, while the Ag/AgCl electrode was employed as the reference electrode, and Pt wire used as the counter electrode. Polarization plots were gained by changing the electrode potential from -1.2 V/REF to + 0.3 V/REF from the open circuit potential (OCP) with a 0.5 mVs^{-1} scan rate. The corrosion parameters were found, in which $I_{corr}$and corrosion potential (E_{corr}) were demonstrated from the intersection of the linear anodic and cathodic branches of Tafel plots and were

determined in the absence and presence of different concentrations of nano-Ag/Ni or nano-Ag/Cu. The corrosion rate (CR) of the various sintered alloys in 3.5% NaCl at room temperature (RT) can be given by the following [21, 22]:

$$CR\ (mm/yr) = \frac{0.00327 * icorr * eq.wt.}{D} \quad (1)$$

where icorr denotes the current density in μA/cm^2, D denotes the specimen density in g/cm^3; eq. wt. denotes the specimen's equivalent weight in grams. The polarization resistance (R_p) values were gained using Stern–Geary Eq. 2:

$$Rp = \frac{\beta a.\beta c}{2.303\ Icorr\ (\beta a+\beta c)} \quad (2)$$

Degrees of surface coverage (θ) in PDP calculations were determined using Eq. 3 [22].

$$\theta = 1 - I_{corr}/\ I_{corr}° \quad (3)$$

where I_{corr} and $I_{corr}°$ denote the corrosion current densities in the AMM reinforced with and without ($SiC+Y_2O_3$) coated with either nano-Ag/Ni or nano-Ag/Cu, respectively.The inhibitive efficiency (IE %) was calculated employing Eq. 4 **[**22].

$$IE\ \% = \theta\ x\ 100 \quad (4)$$

The surface morphology and composition of the corroded AMMCs were examined by SEM and EDX, respectively.

3. Results and discussion

3.1 Powders characterization

A field scanning transmission electron microscope (TEM) was used for the coated powder characterization to investigate the three different metallic coating particles (nano-Ag, nano-Ag/Ni, and nano-Ag/Cu) before the reinforcement powders were mixed with the AMM. Fig. 1 shows the colored scans of the nano-coated layers where the light and dark reds represent the reinforcement particles, which are SiC and Y_2O_3, respectively. The green color represents the first coat layer (nano-Ag) in Fig. 1a, while the green color in Fig. 1b represents the Cu-coated layer, and Fig. 1c represents the coated Ni layer. The Ag-coated layer is not observed in Fig. 1a and 1c which confirms the good coating process of both Cu and Ni on the Ag layer, which makes it completely disappear. The blue color represents the solution in which the samples are immersed. The figure shows a good coating layer of both Ag/Ni and Ag/Cu on the particles with a clear complete capsulation of the SiC and Y_2O_3 particles. This is due to the good electroless chemical deposition parameters, metallization, and sensitization of the coated particles. Many forces affect the adhesion with the witting surface, which are ionic, static polar, and Van der Wall forces. All of them ensure good bonding and consequently good wetting that provides a large contact surface area which assists in the good reinforcement distribution in the matrix and decreases the chance for pore formation.

3.2. Characterization of sintered AMMCs

3.2.1 Relative density

The density of the different AMMC samples was tabulated in Table 1. The highest relative density value is 96.8% for 5% ($SiC+Y_2O_3$)/nano-Ag/Cu samples whereas the lowest value is 95.1% for 7.5% ($SiC+Y_2O_3$)/nano-Ag/Cu samples. The difference between the sintered samples in the densification is very small. This is attributed to the good coating process of the ceramic reinforcement materials with either Cu or Ni which produces a good wettability with the AMM. This helps in decreasing the surface energy between them which causes a good distribution of $SiC-Y_2O_3$ in the AMM with no agglomerations and very low porosity percent [18].

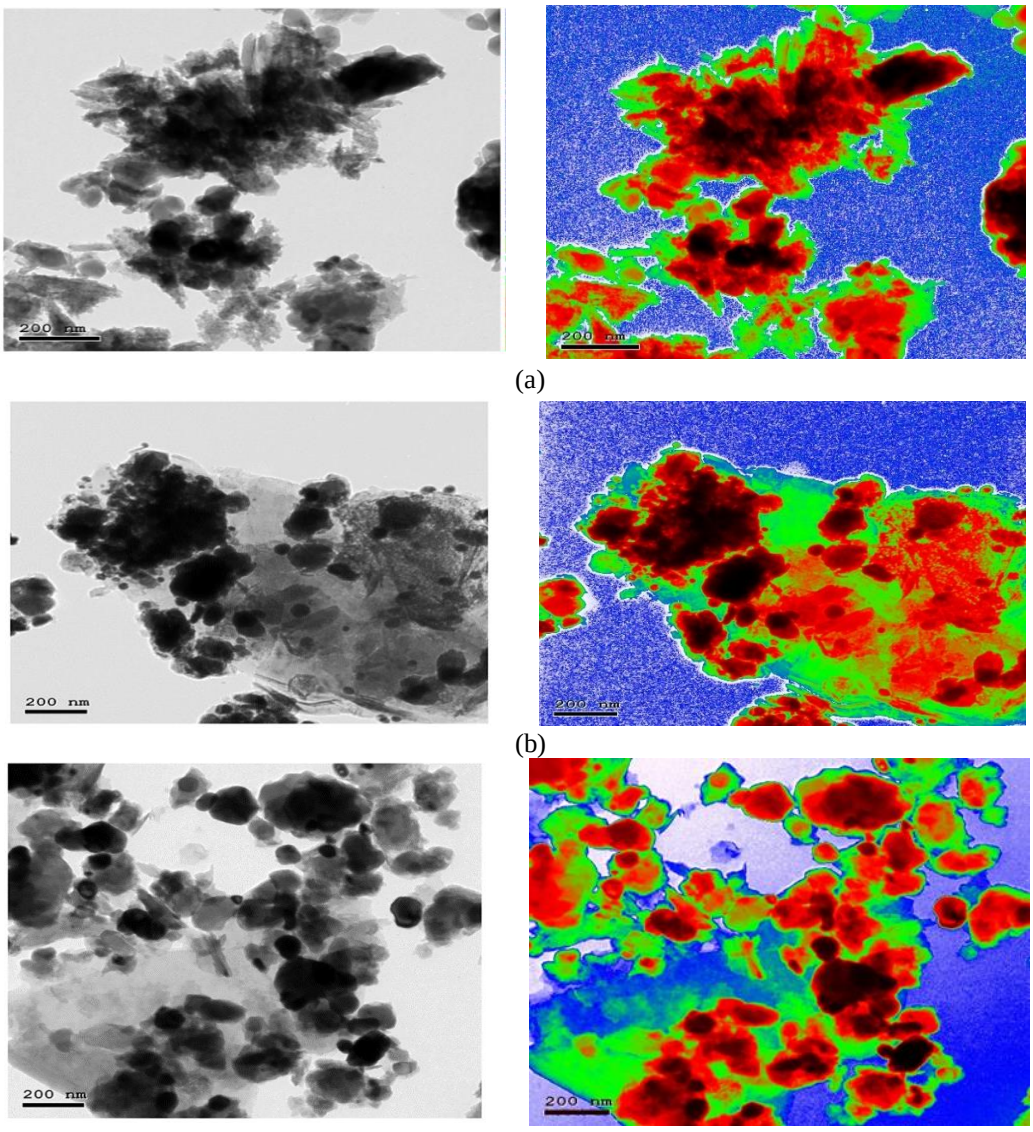

Figure 1: TEM micrographs of ($SiC+Y_2O_3$) powders after coating with (a) nano-Ag, (b) nano-Ag/Cu, and (c) nano-Ag/Ni.

TABLE 1: The different AMMC samples' densities.

AMMCs concentrations	Theoretical density (gm/cm^3)	Actual density (gm/cm^3)	Relative density (%)
Pure Al	2.70	2.59	95.8
2.5% ($SiC+Y_2O_3$) coated nano-Ag/Cu	2.71	2.62	96.7
5% ($SiC+Y_2O_3$) coated nano-Ag/Cu	2.73	2.64	96.8
7.5% ($SiC+Y_2O_3$) coated nano-Ag/Cu	2.75	2.62	95.1
2.5% ($SiC+Y_2O_3$) coated nano-Ag/Ni	2.72	2.62	96.3
5% ($SiC+Y_2O_3$) coated nano-Ag/Ni	2.73	2.61	95.4
7.5% ($SiC+Y_2O_3$) coated nano-Ag/Ni	2.75	2.60	95.8

3.2.2 Wettability

The effect of different coating materials on the interfacial bonding was measured by using a sessile drop test which was conducted on the two group samples. The 5wt%(SiC+Y_2O_3) coated nano-Ag/Cu and 5wt%(SiC+Y_2O_3) coated nano-Ag/Ni samples were chosen for the test since they exhibited better densification and higher hardness compared to the other samples as shown from the upcoming results. The test comprises of placing a drop of water as a wetting liquid on the surface of the sample and measuring the contact angle which in turn gives an indication of the surface energy of the specimen and shows the preferential wetting behavior of the composite [23]. When the contact angle is less than 90° this denotes that the surface has a hydrophilic nature whereas a contact angle of more than 90° means it has a hydrophobic nature. Fig. 2 demonstrated that the nano-Ag/Cu coated sample has a contact angle of 116° whereas the nano-Ag/Ni coated one has a contact angle of 82°, In which the intermolecular forces define the degree of wettability. This indicates that the nano-Ag/Cu coated sample has a more hydrophobic nature than the nano-Ag/Ni coated one which is a result of the good quality of the coating process and indicates that the nano-Ag/Cu coated layer has better coverage over the reinforcement particles than the nano-Ag/Ni layer and a good capsulation of the SiC and Y_2O_3 particles with the nanolayer was achieved. The molecules are pulled to each other due to the cohesion between the molecules. This result is compatible with other results which suggested that the nano-Ag/Ni coating layer did not completely cover the ceramic particles in the matrix. In general, the samples show a good wettability behavior between the coated layer of the particles, with the Al-matrix. This may be due to the addition of yttria which makes the composite surface move towards a hydrophobic nature. It was previously found in other studies that the addition of rare earth oxides changes the polarity of the material surface which in turn changes the surface energy making the composite more hydrophobic [24, 25].

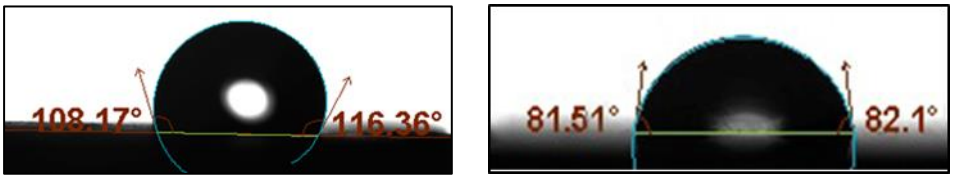

(a) (b)

Figure 2: Contact angle for (a) Al-2.5%(SiC-Y_2O_3) nano-Ag/Cu coated sample and (b) Al-2.5% (SiC-Y_2O_3) nano-Ag/Ni coated sample.

3.2.3 Phase identification

The XRD patterns of pure Al, nano-Ag/Cu, and nano-Ag/Ni coated samples were investigated [19]. The highest peak represents the Al-matrix in both the nano-Ag/Cu and nano-Ag/Ni coated samples as shown in Figs 3 and 4. A peak corresponding to $AlNi_5Si_2$ was recorded due to its formation during the sintering process because of the interaction between the Ni coat, Si, and Al-matrix. This confirms the suggestion of an incomplete Ni coating for some of the reinforcement particles. For the Cu-coated samples, a new phase $AlCu_6$ is detected which means that Cu particles successfully coated the (SiC-Y_2O_3) particles. Furthermore. No oxides were detected because of the vacuum sintering process control. Also, the undesirable Al_4C_3 phase is not detected.

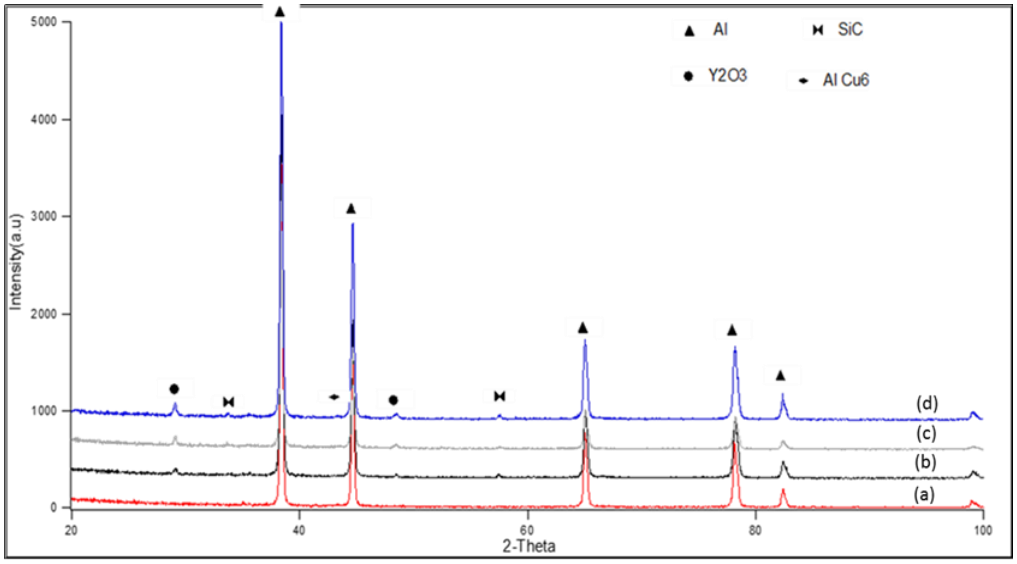

Figure3: The XRD patterns of (a) Al, (b) Al/2.5%(SiC-Y_2O_3)/nano-Ag/Cu, (c) Al/5%(SiC-Y_2O_3)/nano-Ag/Cu, and (d) Al/7.5%(SiC-Y_2O_3)/nano-Ag/Cu [19].

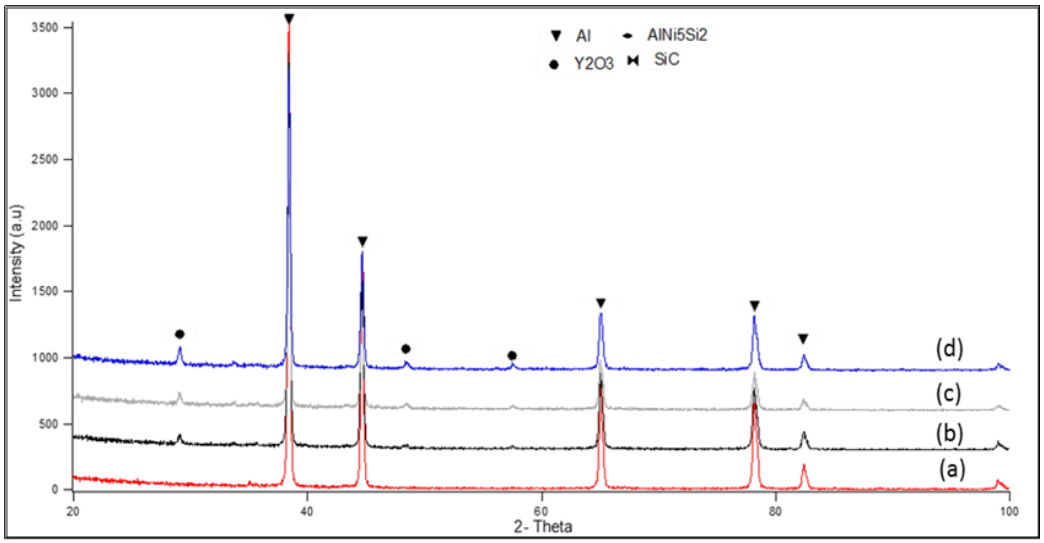

Figure 4: The XRD patterns of (a) Al, (b) Al/2.5%(SiC-Y_2O_3)/nano-Ag/Ni, (c) Al/5%(SiC-Y_2O_3)/nano-Ag/Ni, and (d) Al/7.5%(SiC-Y_2O_3)/nano-Ag/Ni [19].

3.2.3 Microstructure

The micrographs show a uniform distribution of the reinforcement phase (SiC+Y_2O_3)/nano-Ag/Cu or nano-Ag/Ni in the Al-matrix. This is due to the good coating process and efficient fabrication conditions which facilitate the adhesion between the particles and the matrix. Fig. 5 indicates the SEM image of the sintered Al sample whereas Fig. 6 provides the different weight percentages of the reinforcement phase in which a few Y_2O_3 clusters are found. This could be a result of the nano-grained Y_2O_3 which emerged from the milling process. Also, some porosity can be seen in both the nano-Ag/Cu and nano-Ag/Ni coated samples, because of the contrast in the thermal expansion between the reinforcement and the matrix due to their ceramic nature rather than the metallic AMM. The Al has a high coefficient of thermal expansion (CTE) more than SiC and Y_2O_3 which have nearly zero CTE, this causes the

formation of porosity. For the nano-Ag/Cu coated samples shown in Fig. 6, some of the porosity found is mainly located around the reinforcement particles on the interface with the matrix material. In the nano-Ag/Ni coated samples in Fig. 6, the porosity mainly increases with raising the wt% of the reinforcement particles, while simultaneously, the amount of SiC particles visible decreases. This is to the results of the XRD where SiC peaks can be hardly detected and another intermetallic peak is shown. The present observation suggests incomplete coating of the reinforcement particles with nano-Ag/Ni coat which could have led to an interaction between some of the SiC particles and the Al-matrix leading to the $AlNi_5Si_2$ formation and the formation of porosity in the samples. Table 2 indicates the EDX analyses of different sintered AMMC samples.

The effect of coating ceramic particles shows a different particle size with bimodal metallic layers (Ni and Cu) for wettability improvement in AMMC. It was clear that the best results were obtained in the Cu samples rather than Ni-coated ones. Also, some Ni-rich areas were spotted which were due to agglomerations resulting from the separation of the coating layer at some parts [26]. Samples from the same study also featured some debonding at the interface of the Ni-coated SiC particles during tests due to agglomerations and possible air gaps between particles leading to stress concentration at the interfaces [26].

3.2.3 Macro hardness and microhardness

The plastic deformation of the fabricated composite samples was tested using micro and macro-Vickers hardness tests to get more inclusive and accurate values for the bulk material. Table 3 and Table 4 show the microhardness and macro hardness results, respectively. From the two tables, one can notice that all samples coated with nano-Ag/Cu have a higher hardness than those coated with nan0-Ag/Ni, the other notification is that the hardness of the hybrid composites increases with an increase in the reinforcement content as compared to the base metal matrix [27, 28]. Hardness values for both group samples increase gradually with increasing the weight percentage of the reinforcement phase ($SiC+Y_2O_3$) up to 5 wt% and then decrease to 7.5 wt%. This behavior is evident in both tests which indicate good manufacturing parameters. Raising the ceramic phase portion, the hardness values were improved of the AMMC compared to pure Al with values of 132 HV for 5%($SiC+Y_2O_3$)/nano-Ag/Cu sample and 110 HV for 5%($SiC+Y_2O_3$)/nano-Ag/Ni sample compared to 86.5 HV for pure Al. The results show agreement with the densification values and the rule of mixtures**.** The decrease in the hardness values for the 7.5 wt% samples could be a result of the increased porosity as confirmed in the microstructure and density results. Also, the nanoparticles present in the matrix could have led to a second phase hardening effect leading to the increase in the hardness of the samples with increasing the reinforcement in weight percentage. Another observation is that the hardness values for the coated nano-Ag/Cu are higher than those of Ni-coated ones. This could be a result of the successful Cu coat compared to the incomplete coating that occurred in the Ni ones.

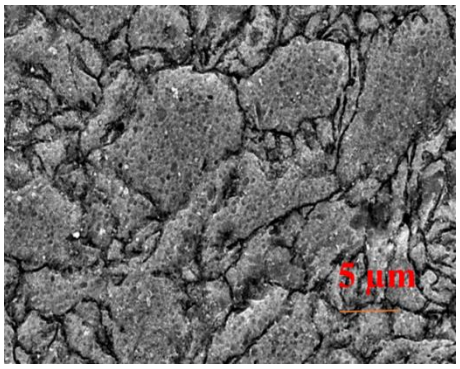

Figure 5: The SEM image of sintered pure Al.

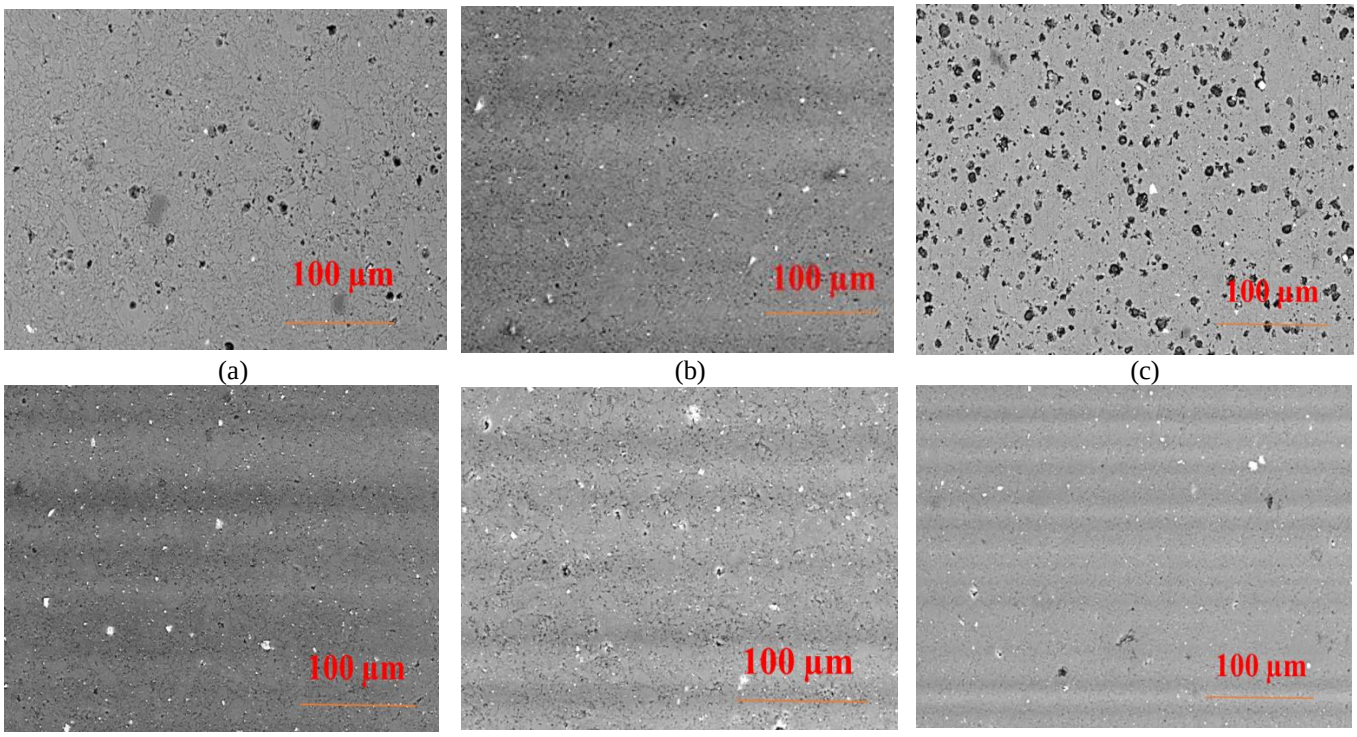

(a) (b) (c)

(d) (e) (f)

Figure 6: The SEM images of different AMMC samples (a) 2.5% (SiC-Y_2O_3)/nano-Ag/Cu, (b) 2.5% (SiC-Y_2O_3)/nano-Ag/Ni, (c) 5.0% (SiC-Y_2O_3)/nano-Ag/Cu, (d) 5.0% (SiC-Y_2O_3)/nano-Ag/Ni, (e) 7.5% (SiC-Y_2O_3)/nano-Ag/Cu, and (f) 7.5% (SiC-Y_2O_3)/nano-Ag/Ni.

TABLE 3: Microhardness for Al/(SiC-Y_2O_3) coated with nano-Ag/Ni or nano-Ag/Cu samples.

AMMCs concentrations	Microhardness (HV)
Pure Al	86.5 ± 3
2.5% (SiC+Y_2O_3) coated nano-Ag/Cu	107.8 ± 4
5% (SiC+Y_2O_3) coated nano-Ag/Cu	132.0 ± 4
7.5% (SiC+Y_2O_3) coated nano-Ag/Cu	121.7 ± 5
2.5% (SiC+Y_2O_3) coated nano-Ag/Ni	98.8 ± 2
5% (SiC+Y_2O_3) coated nano-Ag/Ni	110.0 ± 3
7.5% (SiC+Y_2O_3) coated nano-Ag/Ni	107.7 ± 6

TABLE 4: Hardness for Al/(SiC- Y_2O_3) coated with nano-Ag/Ni or nano-Ag/Cu samples.

AMMCs concentrations	Microhardness (HV)
Pure Al	52 ± 3
2.5% (SiC+Y_2O_3) coated nano-Ag/Cu	76 ± 2
5% (SiC+Y_2O_3) coated nano-Ag/Cu	81 ± 3
7.5% (SiC+Y_2O_3) coated nano-Ag/Cu	79 ± 5
2.5% (SiC+Y_2O_3) coated nano-Ag/Ni	68 ± 3
5% (SiC+Y_2O_3) coated nano-Ag/Ni	76 ± 2
7.5% (SiC+Y_2O_3) coated nano-Ag/Ni	74 ± 4

3.2.4 Wear test

Three different sliding speeds of 0.5, 1.0, and 1.5 m/s were used to study the behavior of different reinforcement in weight percentage at each sliding speed and for each type of coating Cu or Ni. Table 5 shows the average weight loss (mg/m) for each sample. The results are illustrated graphically in Figs 7 and 8. They represent the WR as a function of the weight percentage of the reinforcement coated with Cu and Ni samples respectively at three different sliding speeds 0.5, 1.0, and 1.5 m/s.

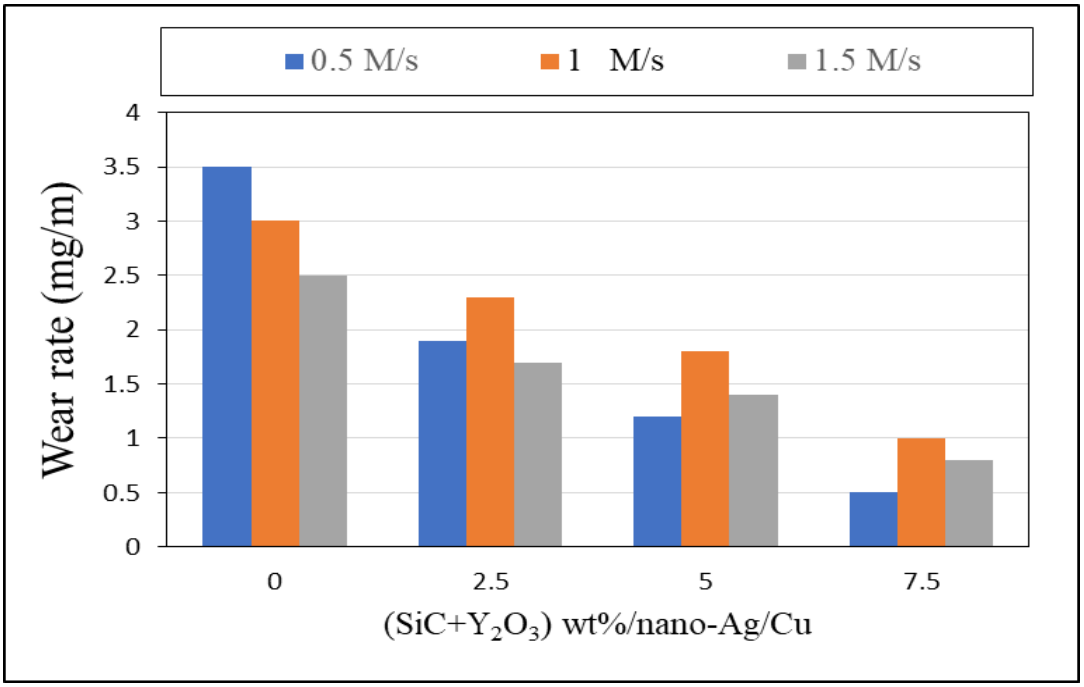

Figure 7: The WR values of sintered Cu-coated samples with different reinforcement percentages.

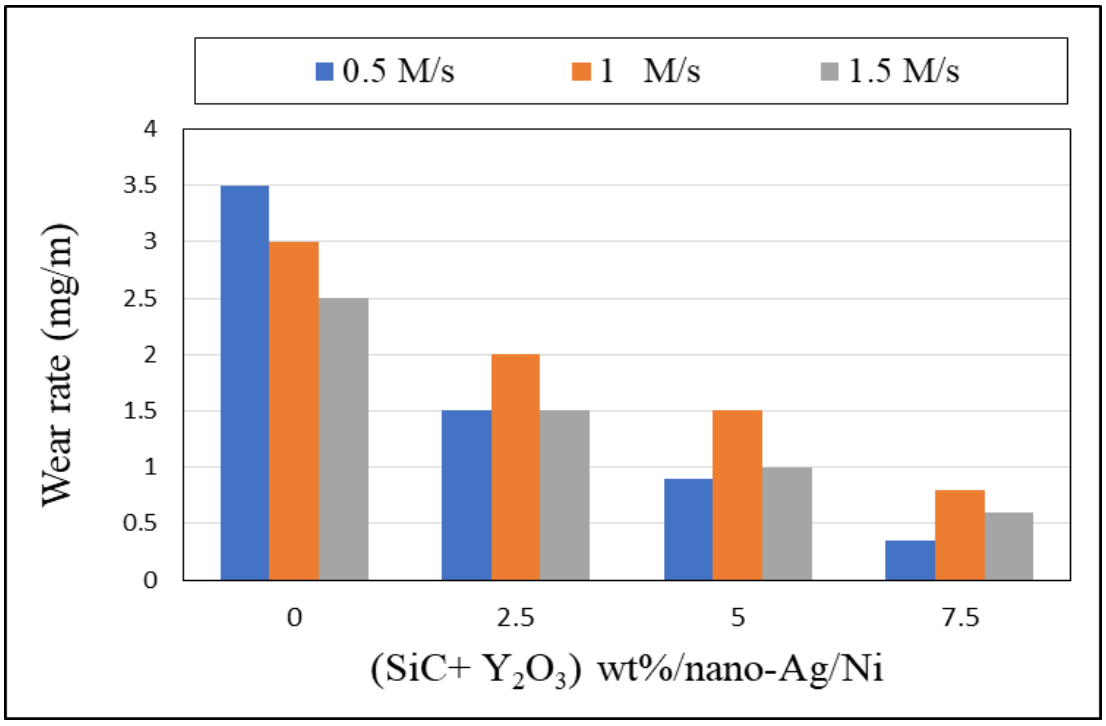

Figure 8: The WR values of sintered Ni-coated samples with different reinforcement percentages.

TABLE5: The WR values of different sintered samples in (mg/s).

AMMCs concentrations	Sliding Speed (m/s)		
	0.5	1.0	1.5
Pure Al	3.5	3.0	2.5
2.5% (SiC+Y_2O_3) coated nano-Ag/Cu	1.9	2.3	1.7
5% (SiC+Y_2O_3) coated nano-Ag/Cu	1.2	1.8	1.4
7.5% (SiC+Y_2O_3) coated nano-Ag/Cu	0.5	1.0	0.8
2.5% (SiC+Y_2O_3) coated nano-Ag/Ni	1.5	2.0	1.5
5% (SiC+Y_2O_3) coated nano-Ag/Ni	0.9	1.5	1.0
7.5% (SiC+Y_2O_3) coated nano-Ag/Ni	0.4	0.8	0.6

From the two figures, one can observe that the WR of Cu samples is higher than Ni ones. From the wetting point of view, it must be obtained another reverse result. As the Cu samples have good wetting and good distribution in the AMM, they must give a better wear resistance. However, the Ni samples recorded the lower recorded lower CR, this can be explained by the incomplete Ni coating on the SiC-Y_2O_3. The surface causes the formation of $AlNiSi_2$ intermetallic which increases the strength of the samples and wear resistance. Its formation during the sintering process has a larger effect on the wear resistance than the wetting effect of Cu samples.

There are three main phenomena from the results. First, the WR decreases with gradual increases in the reinforcement ratio (SiC+ Y_2O_3), and the lowest WR was recorded for the 7.5 wt% of the reinforcement particles. This is observed in both the Cu and Ni-coated samples which indicated that increasing the ceramic phase content improves the overall wear

resistance of the composite material compared to pure Al regardless of the coating type. This is compatible with the previous studies that analyzed the effect of different weight percentages of reinforcement ceramics on the wear behavior of the composite material [24, 28]. Reinforcing a ductile matrix with a hard ceramic phase such as Y_2O_3, and SiC with a good dispersion helps in increasing the wear resistance. All the prepared samples recorded a gradual increase in the WR with increasing the sliding speed up to 1 m/s and decrease again with further increments reaching 1.5 m/s. This may be due to the microthermal softening of the matrix which in turn leads to deterioration in the bonding between the reinforcement particles and the matrix material [29]. With further increase in the sliding speed, a higher temperature was recorded that caused some particles to transfer from the composite to form a thin layer at the worn surfaces. This hard brittle oxide layer called mechanically mixed layer (MML) works as a protective cover and in turn lowers the WR of the composite material [29, 30]. The third observation is that the WR values for the Ni-coated samples are slightly lower than the Cu-coated ones. This could be due to debonding occurring between some SiC particles and the Cu layer during the test. Also, may be attributed to the formed $AlNiSi_2$ intermetallic that was formed during the sintering process, which was detected from the XRD results, this intermetallic has a good effect on the wear resistance. Similar results were found in a previous study where the SiC/Cu interface was found to be weak, and it was the main reason for the deteriorated strength of the composite [17]. This interpretation is consistent with the findings in the microstructure results where some SiC particles were separated from the matrix leaving a few cavities behind that are clear as a pore which hurts the wear resistance. The separation was not due to the unsuccessful coating as shown in the TEM results but rather because of the relatively weaker intermetallic formed at the interface [31, 32]. This could be avoided in future work by introducing an aluminum alloy matrix instead of pure Al.

3.2.5 Electrochemical measurements

The resistance to chemical attacks makes the hybrid reinforced coated AMMCs useful as structural materials for corrosive environments [11]. Many investigations have been done on the corrosion features of AMMCs with Al powder and SiC in 3.5 wt.% NaCl [33]. The effects of SiC particle size and volume fraction on the microstructure and CR of the sintered AMMCs were studied. The AMMCs with SiC reinforced have a lower CR than the pure Al. The CR decline is created by shrinking SiC particles and it increases their volume percentage. The electrochemical examination of Al-Si_{12} as a matrix with a reinforcement of fly ash and carbonized eggshell in 3.5 wt.% NaCl was studied [34]. The results indicate that, as the weight fraction of the reinforcement was increased, the CR of the AMMCs was increased. Few investigations on the decrease of the CR of the unreinforced samples in 3.5 wt.% NaCl than the reinforced AMMCs with wood particles [35]. Also, the CR of AMMCs manufacturing with hybrid reinforcement of SiC and rice husk ash (RHA) was studied with the matrix of Al6063 [36].

Fig. 9 and Fig. 10 represent the PDP curves for the AMMCs with ($SiC+Y_2O_3$) particles coated with nano-Ag/Cu or nano-Ag/Ni in a 3.5 % NaCl solution respectively. All electrochemical parameters are illustrated in Tables 6 and 7 as E_{corr} corrosion potential, I_{corr} corrosion current, R_{pol} polarization

resistance, Tafel slope ßa, ßcanodic and cathodic, respectively. It can be observed from the tables that the CR per year of Cu samples is lower than that of the Ni ones. This may be attributed to the good coating and good contact angle between Cu with SiC and Y_2O_3 more than the Ni samples. This is related to the good wetting properties. The ßa and ßc changed slightly and denoted the influence of Cu or Ni on the kinetics of hydrogen evolution and the AMM-reinforced dissolution. The I_{corr} was obtained from the extrapolation of the Tafel lines (anodic and cathodic) to the corrosion potential. The I_{corr} decreases from 16.039 μAcm^{-2} of blank (pure Al) to 1.33331 μAcm^{-2} with 5%(SiC-Y_2O_3) coated with nano-Ag/Cu and to 1.7079μAcm^{-2} with 7.5%(SiC-Y_2O_3) coated with nano-Ag/Ni. A low I_{corr} value indicates a low CR in a 3.5% NaCl solution [35]. The CR of AMM reinforced is found to be 187.5µm/y and it is minimized by adding different percentages of Cu or Ni reaching a lower value of 15.59µm/y at 5%(SiC-Y_2O_3)/nano-Ag/Cu and 19.97µm/y at 7.5%(SiC-Y_2O_3)/nano-Ag/Ni. The IE is equal to 92 % of optimum concentration 5%(SiC-Y_2O_3)/nano-Ag/Cu and 89 % of optimum concentration 7.5%(SiC-Y_2O_3) coated with nano-Ag/Ni. The CR values of nano-Ag/Cu samples are lower than those of nano-Ag/Ni ones and as the SiC-Y_2O_3 particle percentages increase, the CR was decreased. This may be attributed to more than one phenomenon, the first is the good capsulation and coating of Ag/Cu samples than Ag/Ni. The second is the lower porosity ratio of Ag/Cu which restricted the high contact of the corrosive medium (3.5% NaCl) with the samples. Also, the good distribution of the ceramic reinforcements in the AMM helps in decreasing the CR, due to their high corrosion resistance owing to their ceramic nature and high thermal stability. In this study, the electrochemical behavior was performed on each sample surface and the obtained results are discussed from the detailed microstructure and wettability characters. The surface becomes more hydrophobic with a water contact angle of more than 100º, this helps greatly in improving the distribution of the reinforcement material in the matrix as the hydrophobicity decreases with surface energy and surface tension. This consequently decreases the porosity and so, more electrochemical behavior is established. As a result, the improvement at the corrosion rate of Al-5%(SiC-Y2O3)/coated nano-Ag/Cu and Al-7.5% (SiC-Y_2O_3) coated nano- Ag/Ni are suitable for the aimed application which requires low corrosion rate.

TABLE 6: Corrosion parameters obtained from polarization curves for AMM reinforced with (SiC+Y_2O_3) coated with nano-Ag/Cu in 3.5 % NaCl solution.

AMMCs concentrations	E_{corr} mV	I_{corr} µA/cm²	β_a mV/dec	β_c mV/dec	R_p kohm.cm²	CR µm/Y	θ	IE %
Pure Al	-745.1	16.04	33.3	-46.9	3.51	187.5	--	--
2.5% (SiC+Y_2O_3) coated nano-Ag/Cu	-668.0	3.97	130.3	-146.6	4.09	46.41	0.75	75
5% (SiC+Y_2O_3) coated nano-Ag/Cu	-631.0	1.33	100.8	-196.0	6.14	15.59	0.92	92
7.5% (SiC+Y_2O_3) coated nano-Ag/Cu	-649.0	5.36	86.9	-144.7	2.06	62.66	0.67	67

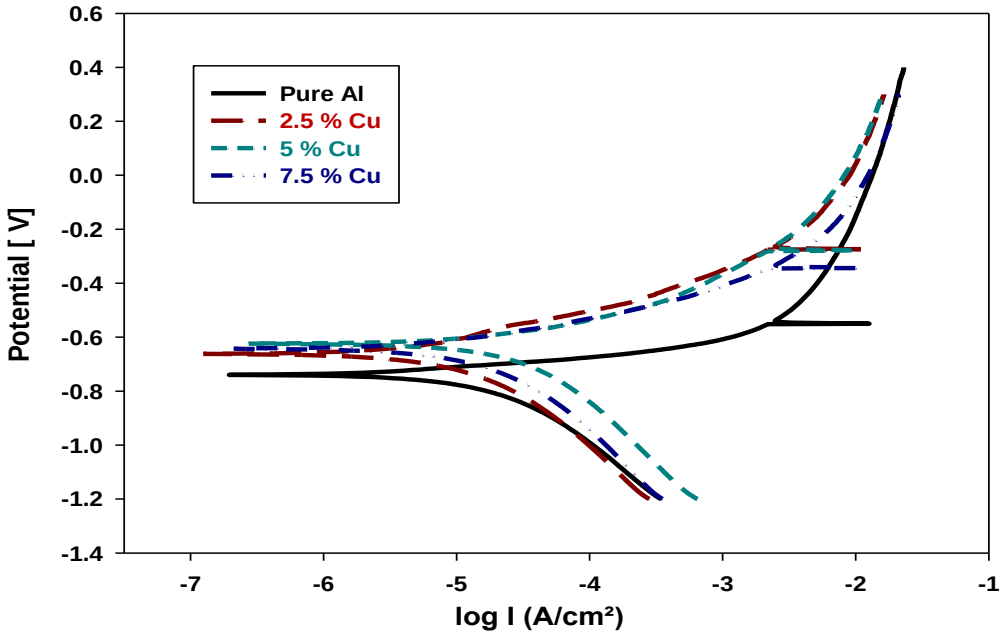

Figure 9: PDP curves for AMM reinforced with ($SiC+Y_2O_3$) coated with nano-Ag/Cu with different coating percentages in 3.5 % NaCl at RT.

TABLE 7: Corrosion parameters obtained from polarization curves for AMM reinforced with ($SiC+Y_2O_3$) coated with nano-Ag/Ni in 3.5 % NaCl.

AMMCs concentrations	E_{corr} mV	I_{corr} µA/cm²	β_a mV/dec	β_c mV/dec	R_p kohm.cm²	CR µm/Y	θ	IE %
Pure Al	-745.1	16.039	33.3	-46.9	3.51	187.50	--	--
2.5% ($SiC+Y_2O_3$) coated nano-Ag/Ni	-655.1	6.864	99.1	-222.4	7.37	80.28	0.572	57
5% ($SiC+Y_2O_3$) coated nano-Ag/Ni	-528.4	3.213	98.6	-328.6	14.80	37.57	0.799	80
7.5% ($SiC+Y_2O_3$) coated nano-Ag/Ni	-660.9	1.708	67.0	-86.4	17.30	19.97	0.893	89

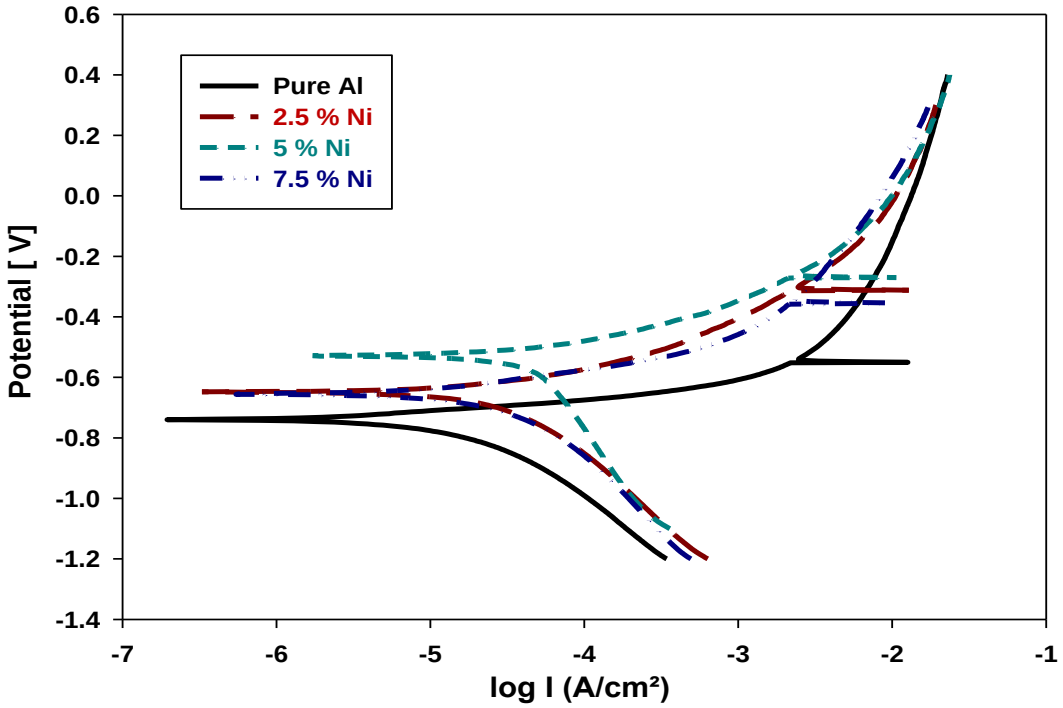

Figure 10: PDP curves for AMM reinforced with ($SiC+Y_2O_3$) coated nano-Ag/Ni with different coating percentages in 3.5 % NaCl at RT.

3.2.2 Surface Morphology

Fig. 11 shows the surface morphology of pure Al, 5%Cu, and 5% Ni samples. Pure Al is the most corroded surface, followed by Ni where the lowest one belongs to Cu samples. From the wetting point of view, the Cu sample has a hydrophobic surface character more than the Ni sample. This gives a good chance for more contact between the particles with a better distribution with fewer agglomerations. So, the lower pores in the Cu samples protect them from high CR, while Ni suffers from porosity formation that increases the CR and affects the surface morphology. The MMC microstructure can affect CR by generating segregation, intermetallic formation, and dislocation creation. Processing deficiencies may induce unexpected forms of corrosion. The electrochemical parameters affecting MMC by the primary MMC constituents, the interphases, chemical degradation in MMCs, the microstructure, and processing [37]. Fig.11 shows the SEM images and Table 8 shows the EDX analysis of pure Al, 5.0%($SiC-Y_2O_3$)/nano-Ag/Cu and 5.0%($SiC-Y_2O_3$)/nano-Ag/Ni. Table 8 gives the EDX results of different corroded AMMC samples. The oxygen percentage is increased for 5.0% ($SiC+Y_2O_3$)/nano-Ag/Ni than 5.0% ($SiC+Y_2O_3$)/nano-Ag/Cu this might be due to higher CR of it as confirmed by the PDP test.

TABLE 8: The EDX of different corroded sintered AMMC samples in wt.%.

AMMCs concentrations	Elements, wt.%							
	Si	C	Y	O	Ag	Cu	Ni	Al
Pure Al	--	--	--	13.9	--	--	--	Bal.
5.0% (SiC+Y_2O_3) coated nano-Ag/Cu	1.3	7.1	0.5	23.8	0.4	6.3	--	Bal.
5.0% (SiC+Y_2O_3) coated nano-Ag/Ni	1.6	6.8	2.6	31.1	--	--	0.4	Bal.

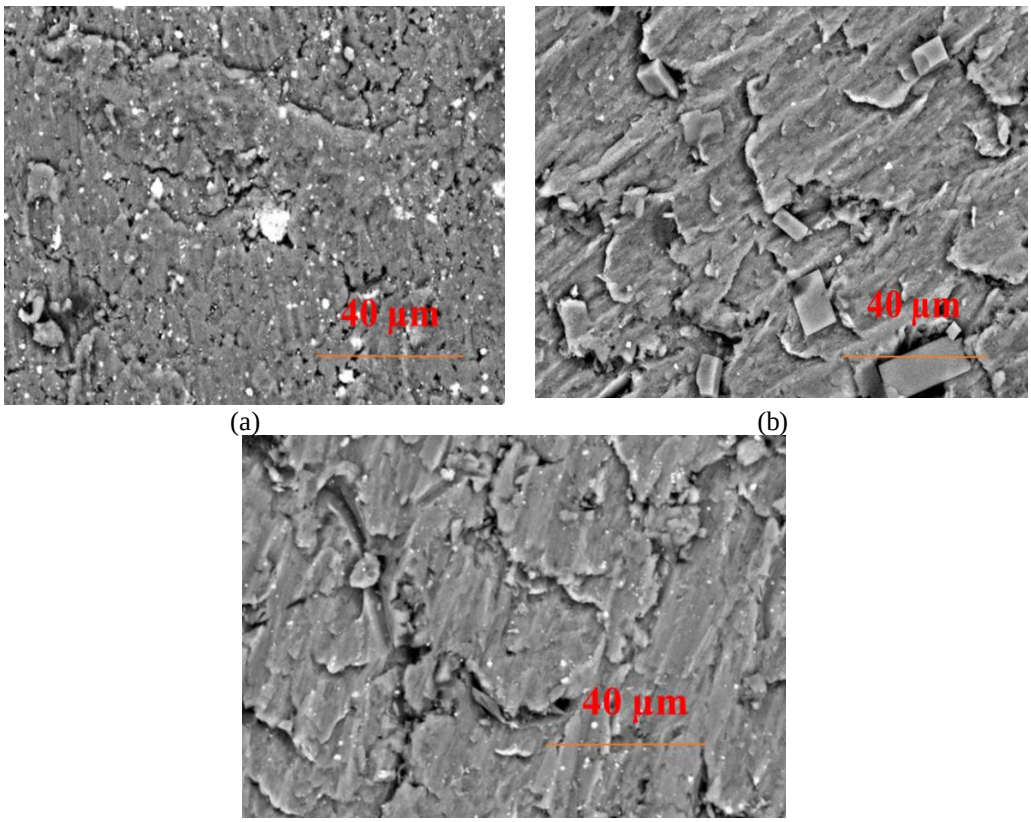

(a) (b)

(c)

Figure 11: Surface morphology of the corroded sintered AMMC samples in 3.5%NaCl where (a) pure Al, (b) 5.0%(SiC-Y_2O_3)/nano-Ag/Cu, and (c) 5.0%(SiC-Y_2O_3)/nano-Ag/Ni.

Conclusions

The significance of all the above results is obtaining AMMCs reinforced with (SiC-Y_2O_3) coated with either nano-Ag/Cu or nano-Ag/Ni with high corrosion and wear resistance which is suitable for spare parts used for sports machines using the electroless chemical deposition technique followed by cold compaction and vacuum sintering. The effect of different weight percentages of the reinforcement phase (SiC- Y_2O_3) (2.5, 5, and 7.5 wt%) on the microstructure, mechanical, and chemical properties of the material was investigated, and the results can be summed up as follows:

1. TEM images showed a complete and uniform Ag/Cu coat layer on the reinforcement particles;

however, the non-uniform coating was observed in Ni-coated samples which is consistent with previous results.

2. Wettability results showed that the Ag/Cu-coated sample had a contact angle of 116 while the Ag/Ni-coated sample was at 82. It indicates that the Ag/Cu-coated sample has a more hydrophobic nature than the Ag/Ni-coated one.
3. The SEM and EDX results showed that the coated reinforcement phase (SiC-Y_2O_3) was uniformly distributed in the AMM. It also showed increased porosity with increasing the wt% of (SiC-Y_2O_3) in the Ag/Ni-coated samples and a decrease in the amount of visible SiC particles which suggests a non-complete coating of Ni on the reinforcement particles.
4. The XRD results confirmed the formation of $AlNi_5Si_2$ peaks observed in the Ni-coated samples evidence of SiC interaction with the AMM. Another $AlCu_6$ peak was visible in the Cu-coated samples which indicates a complete coating of the particles with a Cu-coated layer.
5. It was observed that increasing the wt% content of the reinforcement phase decreases the wear rate (WR) of the composite material with the lowest values at 0.5 m/s sliding speed and 7.5 wt% of reinforcement. At these conditions, the Ni-coated sample had a WR of 0.35 mg/m (90% decrease) and the Ag/Cu-coated sample was at 0.5 mg/m (85% decrease).
6. The inhibiting impact of the AMM reinforced with either nano-Ag/Ni or nano-Ag/Cu in 3.5% NaCl solution was studied potentiodynamic polarization (PDP). It was found that the AMM reinforced with nano-Ag/Cu-coated acts as a good mixed-type corrosion inhibitor. The corrosion rate (CR) decreases with increasing the reinforced either nano-Ag/Ni or nano-Ag/Cu.
7. The CR of Al-matrix reinforced is found to be 187.5 µm/y and it is minimized by adding different percentages of Cu or Ni reaching a lower value of 15.59 µm/y at 5%(SiC-Y_2O_3)/nano-Ag/Cu, and 19.97 µm/y at 7.5%(SiC-Y_2O_3)/nano-Ag/Ni.
8. In addition, the sample reinforced with 5%(SiC-Y_2O_3)/nano-Ag/Cu, and 7.5%(SiC-Y_2O_3)/nano-Ag/Ni-coated showed a better corrosion resistance than another percentage. The low CR to other reinforced samples is because of the small amount of SiC reinforcement.

Competing interests

The authors declare that they have no conflicts of interest.

References

1. S. Gururaja, M. Ramulu, W. Pedersen, Machining of MMCs: A review, Machining Science and Technology, 17:41–73 (2013)
2. S. Natarajan, R. Narayanasamy, S. P. Kumaresh Babu, G. Dinesh, B. Anil Kumar, K. Sivaprasad, Sliding wear behaviour of Al 6063/TiB2 in situ composites at elevated temperatures, Mater. Des., 30(7) (2009) 2521–2531.
3. Y. Sahin, "Preparation and some properties of SiC particle reinforced aluminium alloy composites," Mater. Des., 24 (2003) 671–679
4. T. Ozben, E. Kilickap, and C. Orhan, Investigation of mechanical and machinability properties of SiC particle reinforced Al-MMC, J. Mater. Process. Technol., 198(1–3) (2008) 220–225.
5. N. Beigi Khosroshahi, R. Azari Khosroshahi, R. Taherzadeh Mousavian, D. Brabazon, Electroless

deposition (ED) of copper coating on micron-sizedSiC particles," Surf. Eng., 30(10) (2014) 747–751.

6. A. V. Muley, S. Aravindan, I. P. Singh, Nano and hybrid aluminum based metal matrix composites: An overview, Manuf. Rev., 2 (2015).
7. M. O. Bodunrin, K. K. Alaneme, L. H. Chown, Aluminium matrix hybrid composites: A review of reinforcement philosophies; Mechanical, corrosion and tribological characteristics, J. Mater. Res. Technol., 4(4) (2015) 434–445.
8. M. Patel, S.K. Sahu, M.K. Singh, Fabrication and Investigation of Mechanical Properties of SiC Particulate Reinforced AA5052 Metal Matrix Composite,
   J. Mod. Mater.; 7(1), (2020) 26-36
9. S. Ozden, R. Ekici, and F. Nair, "Investigation of impact behaviour of aluminium based SiC particle reinforced metal–matrix composites," Compos. Part A Appl. Sci. Manuf., 38 (2007) 484–494.
10. M. Megahed, M. A. Attia, M. Abdelhameed, A. G. El-Shafei, Tribological characterization of hybrid metal matrix composites processed by powder metallurgy, Acta Metall. Sin. (English Lett.), 30(8) (2017) 781–790.
11. J. A. Voigt, An integrated study of the ceramic processing of yttria, 1986.
12. R. Kheirifard, N. Beigi Khosroshahi, R. Azari Khosroshahi, R. Taherzadeh Mousavian, D. Brabazon, Fabrication of A356-based rolled composites reinforced by Ni–P-coated bimodal ceramic particles, Proc. Inst. Mech. Eng. Part L J. Mater. Des. Appl., 232(10) (2018) 803–815.
13. H. Ahamed, V. Senthilkumar, Role of nano-size reinforcement and milling on the synthesis of nano-crystalline aluminium alloy composites by mechanical alloying," J. Alloys Compd., 505(2) (2010) 772–782.
14. S. F. Hassan, M. Gupta, Effect of different types of nano-size oxide particulates on microstructural and mechanical properties of elemental Mg, J. Mater. Sci. 4(8) (2006) 2229–2236.
15. H. Ahamed, V. Senthilkumar, Consolidation behavior of mechanically alloyed aluminum based nanocomposites reinforced with nanoscale Y_2O_3/Al_2O_3 particles," Mater. Charact., 12(62) (2011) 1235–1249.
16. L. Luo, J. Yu, J. Luo, J. Li, Preparation and characterization of Ni-coated Cr_3C_2 powder by room temperature ultrasonic-assisted electroless plating, Ceram. Int., 36(6) (2010) 1989–1992.
17. D. M. Jarząbek, C. Dziekoński, W. Dera, J. Chrzanowska, T. Wojciechowski, Influence of Cu coating of SiC particles on mechanical properties of Ni/SiC co-electrodeposited composites, Ceram. Int., 44(17) (2018) 21750–21758.
18. S. A. Abolkassem, O. A. Elkady, A. H. Elsayed, W. A. Hussein, H. M. Yehya, Effect of consolidation techniques on the properties of Al matrix composite reinforced with nano Ni-coated SiC, Results Phys., 9 (2018) 1102–1111.
19. G. Fadel, L.Z. Mohamed, O.A. Elkady, A.A. Elhabak, M. A. Adly, S. A. Abolkassem, Studying the Microstructure, Physical and Mechanical Properties of Al Matrix Reinforced with Bi-Modal Particles Coated with Either Ni or Cu, Trans Indian Inst Met, 2022
20. S. Tahamtan, A. Halvaee, M. Emamy, M. S. Zabihi, Fabrication of Al/A206-Al2O3 nano/micro composite by combining ball milling and stir casting technology, Mater. Des., 49 (2013) 347–359.

21. G.A. Gaber, A. Abdelfattah., L.Z. Mohamed, A comprehensive investigation of corrosion efficiency of Cu-10Ni alloy in hybrid Cr3+/Ni2+ with tungstate in chloride media, Egypt. J. Chem., (2024)
22. G.A. Gaber, L.Z. Mohamed, A. Abdelfattah, Study the corrosion issues on galvanized steel induced in water tanks, Chemical Papers (2023) 77:7539–7549
23. T. P. D. Rajan, R. M. Pillai, B. C. Pai, Reinforcement coatings and interfaces in aluminium metal matrix composites, J. Mater. Sci. 33(14) (1998) 3491–3503.
24. V. K. Sharma, V. Kumar, R. S. Joshi, Parametric study of aluminium-rare earth based composites with improved hydrophobicity using response surface method, J. Mater. Res. Technol., 9(3) (2020) 4919–4932.
25. N. Shao, J. W. Dai, G. Y. Li, H. Nakae, T. Hane, Effect of La on the wettability of Al2O3 by molten aluminum," Mater. Lett., 58(14) (2004) 2041–2044.
26. Y. Afkham, S. M. Fattahalhoseini, R. A. Khosroshahi, C. Avani, N. Mehrooz, R. T. Mousavian, "Incorporation of Silicon Carbide and Alumina Particles into the Melt of A356 via Electroless Metallic Coating Followed by Stir Casting," Silicon, 10(5) (2018) 2353–2359.
27. A. Awasthi, N. Panwar, A. S. Wadhwa, A. Chauhan, Mechanical Characterization of hybrid aluminium Composite-A review, Mater. Today Proc., 5(14) (2018) 27840–27844.
28. H. Herzallah, A. Elsayd, A. Shash, M. Adly, Effect of carbon nanotubes (CNTs) and silicon carbide (SiC) on mechanical properties of pure Al manufactured by powder metallurgy, J. Mater. Res. Technol., (2019) 4–10.
29. G. B. V. Kumar, C. S. P. Rao, N. Selvaraj, Mechanical and Tribological Behavior of Particulate Reinforced Aluminum Metal Matrix Composites – a review, J. Miner. Mater. Charact. Eng., 10(1) (2011) 59–91.
30. A. Moosa, A. Yass, Effect of Rare Earth Addition on Wear Properties of Aluminum Alloy- Rice Husk Ash/Yttrium Oxide Hybrid Composites, 2016.
31. J. Islam, Hasan-ur-Rahman, H.M. Al Rashed, The Effect of Magnesium and Heat Treatment on the Hardness as well as Microstructures of Aluminium Copper Binary Alloys, Int. J. Eng. Adv. Technol., 2017
32. G. Mathers, The welding of aluminium and its alloys. CRC Press, 2002.
33. H.M. Zakaria, Microstructural and corrosion behavior of Al/SiC metal matrix composites. Ain. Shams. Eng. J. 2014, 5, 831–838.
34. N. Ononiwu, C. Ozoegwu, N. Madushele, O.J. Akinribide, Mechanical Properties Tribology and Electrochemical Studies of Al/Fly Ash/Eggshell Aluminium Matrix Composite. Biointerface Res. Appl. Chem. 2022, 12, 4900–4919
35. M. Oki, A. Adeleke, O. Adesina, P. Omoniyi, E. Akinlabi, Electrochemical Studies of the Corrosion Behavior of Al/SiC/PKSA Hybrid Composites in 3.5% NaCl Solution Peter Ikubanni, J. Compos. Sci., 6, (2022) 286.
36. R. Haridass, N. Vishnu, A. Abinesh, K.N. Manoj, Determination of corrosion behaviour of Al6063-SiC-RHA metal matrix composites. Int. J. Pure Appl. Math., 118, (2018) 907–915.
37. W.A. Wesley, R.H. Brown, The Corrosion Handbook, 1st ed; Uhlig, H. H., Ed.; Wiley: New York, 1948; 481–495.